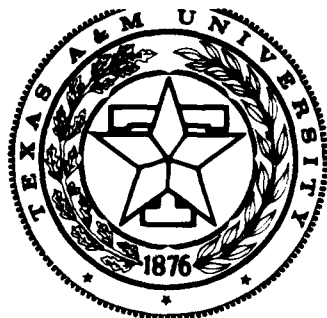


AD-A197 500

DTIC FILE COPY



Mechanics and Materials Center
TEXAS A&M UNIVERSITY
College Station, Texas

ON THE MECHANICS OF CRACK CLOSING AND BONDING
IN LINEAR VISCOELASTIC MEDIA

R.A. SCHAPERY

DTIC
ELECTE
JUL 26 1988
S D

OFFICE OF NAVAL RESEARCH
DEPARTMENT OF THE NAVY
CONTRACT N00014-86-K-0298
WORK UNIT 4324-520

DISTRIBUTION STATEMENT A

Approved for public release
Distribution Unlimited

MM 5488-88-6

JULY 1988

unclassified

SECURITY CLASSIFICATION OF THIS PAGE

REPORT DOCUMENTATION PAGE

1a. REPORT SECURITY CLASSIFICATION unclassified		1b. RESTRICTIVE MARKINGS													
2a. SECURITY CLASSIFICATION AUTHORITY		3. DISTRIBUTION/AVAILABILITY OF REPORT unlimited													
2b. DECLASSIFICATION/DOWNGRADING SCHEDULE															
4. PERFORMING ORGANIZATION REPORT NUMBER(S) MM 5488-88-6		5. MONITORING ORGANIZATION REPORT NUMBER(S)													
6a. NAME OF PERFORMING ORGANIZATION Mechanics & Materials Center Texas A&M University	6b. OFFICE SYMBOL (If applicable)	7a. NAME OF MONITORING ORGANIZATION ONR													
6c. ADDRESS (City, State and ZIP Code) College Station, Texas 77843		7b. ADDRESS (City, State and ZIP Code)													
8a. NAME OF FUNDING/SPONSORING ORGANIZATION ONR	8b. OFFICE SYMBOL (If applicable)	9. PROCUREMENT INSTRUMENT IDENTIFICATION NUMBER Contract N00014-86-K-0298													
8c. ADDRESS (City, State and ZIP Code) Mechanics Division Office of Naval Research/Code 1513A:DLW 800 N. Quincy Avenue Arlington, VA 22217-5000		10. SOURCE OF FUNDING NOS. <table border="1"><thead><tr><th>PROGRAM ELEMENT NO.</th><th>PROJECT NO.</th><th>TASK NO.</th><th>WORK UNIT NO.</th></tr></thead><tbody><tr><td></td><td></td><td></td><td>4324-520 (4327-814)</td></tr></tbody></table>		PROGRAM ELEMENT NO.	PROJECT NO.	TASK NO.	WORK UNIT NO.				4324-520 (4327-814)				
PROGRAM ELEMENT NO.	PROJECT NO.	TASK NO.	WORK UNIT NO.												
			4324-520 (4327-814)												
11. TITLE (Include Security Classification) On the Mechanics of Crack Closing and Bonding in Linear Viscoelastic Media															
12. PERSONAL AUTHOR(S) R.A. Schapery															
13a. TYPE OF REPORT Technical	13b. TIME COVERED FROM _____ TO _____	14. DATE OF REPORT (Yr., Mo., Day) July 1988	15. PAGE COUNT												
16. SUPPLEMENTARY NOTATION															
17. COSATI CODES <table border="1"><thead><tr><th>FIELD</th><th>GROUP</th><th>SUB. GR.</th></tr></thead><tbody><tr><td></td><td></td><td></td></tr><tr><td></td><td></td><td></td></tr><tr><td></td><td></td><td></td></tr></tbody></table>		FIELD	GROUP	SUB. GR.										18. SUBJECT TERMS (Continue on reverse if necessary and identify by block number) JES	
FIELD	GROUP	SUB. GR.													
19. ABSTRACT (Continue on reverse if necessary and identify by block number) The mechanics of quasi-static crack closing and bonding of surfaces of the same or different linear viscoelastic materials is described. Included is a study of time-dependent joining of initially curved surfaces under the action of surface forces of attraction and external loading. Emphasis is on the use of continuum mechanics to develop equations for predicting crack length or contact size as a function of time for relatively general geometries; atomic and molecular processes associated with the healing or bonding process are taken into account using a crack tip idealization which is similar to that used in the Barenblatt method for fracture. Starting with a previously developed correspondence principle, an expression is derived for the rate of movement of the edge of the bonded area. The effects of material time-dependence and the stress intensity factor are quite different from those for crack growth. A comparison of intrinsic and apparent energies of fracture and bonding is made, and criteria are given for determining whether or not bonding can occur. Examples are given to illustrate use of the basic theory for predicting healing of cracks and growth of															
20. DISTRIBUTION/AVAILABILITY OF ABSTRACT UNCLASSIFIED/UNLIMITED <input checked="" type="checkbox"/> SAME AS RPT. <input type="checkbox"/> DTIC USERS <input type="checkbox"/>		21. ABSTRACT SECURITY CLASSIFICATION													
22a. NAME OF RESPONSIBLE INDIVIDUAL Dr. Richard L. Miller, Code 1132P		22b. TELEPHONE NUMBER (Include Area Code) (202) 696-4405	22c. OFFICE SYMBOL												

contact area of initially curved surfaces. Finally, the affect of bonding time on joint strength is estimated from the examples on contact area growth.



On The Mechanics of Crack Closing and
Bonding in Linear Viscoelastic Media

R.A. Schapery

Civil Engineering Department

Texas A&M University

College Station, TX 77843

Accession For	
NTIS CRA&I	<input checked="checked" type="checkbox"/>
DTIC TAB	<input type="checkbox"/>
Unannounced	<input type="checkbox"/>
Justification	
By	
Distribution/	
Availability Codes	
Dist	Avail and/or Special
A-1	

ABSTRACT

The mechanics of quasi-static crack closing and bonding of surfaces of the same or different linear viscoelastic materials is described. Included is a study of time-dependent joining of initially curved surfaces under the action of surface forces of attraction and external loading. Emphasis is on the use of continuum mechanics to develop equations for predicting crack length or contact size as a function of time for relatively general geometries; atomic and molecular processes associated with the healing or bonding process are taken into account using a crack tip idealization which is similar to that used in the Barenblatt method for fracture. Starting with a previously developed correspondence principle, an expression is derived for the rate of movement of the edge of the bonded area. The effects of material time-dependence and the stress intensity factor are quite different from those for crack growth. A comparison of intrinsic and apparent energies of fracture and bonding is made, and criteria are given for determining whether or not bonding can occur. Examples are given to illustrate use of the basic theory for predicting healing of cracks and growth of contact area of initially curved surfaces. Finally, the affect of bonding time on joint strength is estimated from the examples on contact area growth.

1. Introduction

In 1966 Williams [1] observed that "... adhesive failure is not normally analyzed as a fracture problem in continuum mechanics." He then demonstrated that cohesive and adhesive fracture may be analyzed by similar methods through consideration of the stress singularity at crack tips and an energy balance. Following this pioneering paper the understanding of adhesive failure has advanced greatly, clearly aided by the use of fracture mechanics theory as urged by Williams.

Quasi-static analysis of adhesive and cohesive fracture of linear viscoelastic media has also reached a relatively mature state through application of fracture mechanics principles [e.g., 2-7]. There are, however, still important unsolved problems of cohesive and adhesive fracture of nonhomogeneous media; in many cases the stresses on the crack plane are functions of the local viscoelastic properties, which significantly complicates the analysis [5,8]. Much progress has been made as well on dynamic fracture of linear homogeneous viscoelastic materials by Walton [9], among others; at sufficiently high crack speeds the stresses depend on viscoelastic properties.

The problem which is the opposite of fracture, the bonding of surfaces, has received far less attention in the context of fracture-like mechanics. For elastic media under quasi-static conditions, the analysis of bonding is essentially the same as that of fracture. Johnson et al. [10] and Roberts and Thomas [11] studied by experiment and linear theory the bonding and unbonding of flat and curved surfaces of rubber with other materials. They used energy methods analogous to those employed in elastic fracture mechanics, recognizing that contact mechanics and fracture mechanics have to be combined. Although some viscoelastic effects were observed, essentially elasticity theory was

used. Later, Greenwood and Johnson [12] made a viscoelastic fracture analysis of the separation of a sphere from a plane, allowing for dissimilar materials, but assuming there are no shear stresses along the interface. The force of attraction acting across the interface was based on a theoretical model of the force between planes of atoms as a function of separation distance.

In a series of six papers, Anand and coworkers [13-18] studied the so-called problem of autohesion, which is the bonding of surfaces of the same material. Contact area growth between irregular (locally curved) surfaces was analyzed using linear viscoelastic contact mechanics. The influence of the force of attraction between surfaces was implicitly neglected compared to that due to a constant externally applied compression when predicting contact area growth. The increase of tensile joint strength with contact time was assumed to be due to the area increase. Other studies of polymer-polymer bonding have assumed complete contact is achieved immediately, and the time-dependence of strength is due to interdiffusion of molecular segments across the interface and the related formation of entanglements; many references may be found in the recent paper on crack healing by Kausch et al. [19]. Jud et al. [20] and Stacer and Schreuder-Stacer [21] discussed the time-dependence of the wetting or contact process in comparison to that for interdiffusion; some explicit estimates of contact time-dependence are in [20].

In this paper we address the problem of bonding between linear, isotropic viscoelastic media, accounting for the affect of interfacial forces of attraction (or surface energy) and external loading on the rate of growth of bonded area. Processes are assumed to occur slowly enough that inertia effects are negligible and, also for simplicity, we consider only the mode I problem (in which only normal stresses act across the bond surface). The theory shows how crack healing and contact area growth may occur under either

external tensile or compressive forces, and a relatively simple method is developed for predicting this behavior.

It is believed the results will be useful for the development of basic models of the healing of damage in composites, insofar as this damage consists of micro- or macrocracks. Significant amounts of healing have been observed experimentally for asphalt [22] and solid propellant [23], which are particulate composites. More generally, the theory may be used to account for viscoelasticity and surface force or energy effects in adhesion and autohesion processes when externally applied compression is not large enough to produce complete, immediate surface-to-surface contact. Although the surface energy may be small, over a long period of time it can produce considerable deformation and contact area growth in soft materials. With a minor modification the theory in this paper would provide a means for predicting the effect of a concentrated shear stress at the trailing edge of so-called "waves of detachment" observed in the sliding of rubber on smooth surfaces [24]; addition of an interfacial shear stress may be done in the same way as described in [5] for fracture.

In order to illustrate the type of behavior studied here, consider the problem in Figure 1. Figure 1a shows the affect of (positive) surface energy on the contact between a deformable spherical surface and a rigid flat surface. Without surface energy, Fig. 1b, the spherical surface is tangent to the flat surface at the contact edge, and the load necessary to produce contact to the radius a_c is given by the Hertz theory [25]. Less compressive force is needed in Fig. 1a for the same contact radius; indeed, with surface energy a tensile force can be supported. The dashed lines in Fig. 1 indicate the positions of undeformed spherical surfaces after experiencing the same amount of movement at the remote loading point as in the deformed body. When

the body is viscoelastic, the contact radius varies with loading rate and, at the same load, may be considerably different for positive bonding speed ($\dot{a}_c > 0$) than for debonding or crack growth ($\dot{a}_c < 0$). With a small tensile or zero external force, the interfacial force of attraction acting across the cusp-shaped separation at the contact edge causes the contact radius to grow; if the long-time modulus of the sphere is zero (e.g., noncrosslinked rubber) the contact will grow indefinitely, just as for a liquid. The force required to separate totally the two bodies may be large if considerable viscoelastic dissipation accompanies the separation process. The separation process was analyzed by Greenwood and Johnson [12] using the author's theory of crack growth [4]. Here, a theory is developed for predicting the viscoelastic bonding process for this and other geometries and material combinations, as well as for healing of internal cracks.

Section 2 introduces the notation and geometry used in describing the edge of the bonded area. This edge region, Fig. 2, is assumed to be very small compared to the contact size; for example, it exists only at the contact edge in Fig. 1a where the parabolic surface profile touches the lower flat plate. Without the local tangential separation shown in Fig. 2, the stresses at the contact edge would be infinite, according to linear viscoelasticity theory. With edge movement, these infinite stresses produce infinite strain rates and lead to physically unacceptable predictions of bonding or crack speed. In the latter case, it is well-known that the singular stresses lead to a physically unacceptable prediction of crack growth. Difficulties arising from use of the classical singular stresses were recognized by Williams [2], who circumvented the problem by replacing the local geometry of a crack by a spherical flaw. Later, Knauss [3] and the author [4] used the Barenblatt method (or what is often called the Dugdale-Barenblatt or Dugdale method) to

remove the singularity. The latter approach is used in this paper; it amounts to adjusting δ and/or σ_b so that the stresses on the bond surface (and in the continua) are finite.

Section 3 indicates how the stresses and displacements in viscoelastic media may be obtained from elastic solutions. This approach is used in Section 4 with Barenblatt's method for elastic media to obtain the local viscoelastic interfacial stress and displacement. In contrast to the crack growth problem, the stresses in elastic and viscoelastic bodies are different. This difference complicates the bonding problem, and leads to viscoelastic effects in the neighborhood of the bond edge which are considerably different than predicted with crack growth. Nevertheless, in certain cases it is possible to derive relatively simple equations for predicting bonding speed and the bonding-zone length δ , Fig. 2, in terms of the stress intensity factor. In Section 5 the interface bonding stress σ_b , Fig. 2, is assumed constant, and exact expressions are obtained for a material characterized by a generalized power law creep compliance; approximate expressions are then developed for a more general form of creep compliance. In the Appendix a simple power law compliance is used with a bonding stress σ_b that varies with distance between the surfaces to derive an exact equation for bonding speed; the dependence of bonding speed on stress intensity factor is found to be the same as for constant σ_b . Section 6 is concerned with the energy needed for crack growth as compared to that for bonding of surfaces, accounting for viscoelastic dissipation effects. Examples of crack healing and the bonding of initially curved surfaces are given in Section 7, using the theory developed in Section 5. The theory can be readily extended to certain types of orthotropic linear and nonlinear media, as discussed in the concluding remarks in Section 8.

2. Description of the contact edge

Referring to Fig. 2, the (x,y) coordinate system is stationary, with the y -axis located at any convenient position in the continuum; $y = 0$ defines the surface along which bonding occurs. We assume this surface is locally flat, but do not restrict its shape far from the contact edge (relative to a). The bodies above and below $y = 0$ are assumed to be in contact to the right of the point designated as P . In practice, surface irregularities may prevent complete contact of the adjacent areas; however, for our purposes, it will be sufficient to assume only that the scale of this local roughness is small compared to the length of the bonding zone a which is defined below.

To the left of the position $x = a - b$ the two surfaces are assumed to be far enough apart that the intermolecular force of attraction is negligible. Over the length a the force of attraction, which on the scale of the continuum is represented by the tensile bonding force per unit area, σ_b , tends to draw the adjacent surfaces together until complete contact exists (in the sense indicated earlier).

The edge of complete contact (which can also be thought of as a crack tip), whose intersection with the plane of the page is the point P , is in general a curved line in space which may be closed or else open and ending on the edges of the continuum. It is necessary to assume the radius of curvature of this line in the neighborhood of the point P is large relative to a in order to be able to use the equations of plane strain in a local bonding analysis; this neighborhood is defined by the size a .

The materials above and below the bond surface are assumed to be linearly viscoelastic, homogeneous and isotropic, with the possible exception of a thin surface layer of damaged material; this layer, which may be the result of the

surface being formed in the first place by means of crack growth or any other process, will have no practical affect on our analysis if its thickness is small compared to δ . As noted previously, the scale of local surface roughness is similarly assumed to be small. These surface features will, of course, affect the particular values of σ_b which are to be used in the theory. Roughness on a scale much larger than δ is permitted.

3. Viscoelastic stresses and displacements

By following arguments based on the Laplace transform similar to those given in [4] for the case of the opening mode of crack growth, we can express viscoelastic stresses and displacements in terms of elastic solutions for crack shortening; this approach amounts to the use of the extended correspondence principle for contact or indentation problems [6].

With crack growth or no growth, i.e. $\dot{a} \geq 0$ in Fig. 2, the normal stress acting along the plane of crack prolongation is the same for both elastic and viscoelastic bodies (which are assumed to be identical with respect to geometry and applied loads) if this stress for the elastic body is independent of elastic constants. This result in turn leads to viscoelastic displacements which can be written explicitly in terms of the history of the elastic values.

In contrast, it may be shown by using the Laplace transform that with crack shortening (or, equivalently, in problems with growing contact area) the normal displacements and stresses take on opposite roles with respect to elastic solutions if the elastic normal surface displacement is independent of the elastic constants. This latter condition is not necessarily satisfied for the type of boundary value problems of interest here unless the Poisson's ratio is constant and all traction boundary conditions are converted to specified displacement boundary conditions. When the Poisson's ratio is constant (or, at least, the effect of its time-dependence is small enough that

it may be assumed constant) the more straightforward method given in [26] for constructing viscoelastic solutions from elastic solutions may be used. The method is not based on Laplace transform theory although it uses a so-called correspondence principle, designated as CP-III in [26]. This correspondence principle may be used with certain types of nonlinearity (including distributed damage), anisotropy, and aging. However, for simplicity we consider here only linear, isotropic, nonaging media.

Let us now state the relevant version of CP-III and then define the terms:

If $\partial n_i / \partial t = 0$ on the surface S_T and $dS_T/dt \leq 0$, the viscoelastic solution is

$$\sigma_{ij} = (E d \sigma_{ij}^R) \quad (1)$$

$$u_j = u_j^R \quad (2)$$

where σ_{ij}^R and u_j^R satisfy the field equations and boundary conditions of the so-called reference elastic problem (or, more briefly, the elastic problem) defined below.

The viscoelastic and elastic bodies are assumed to be geometrically identical in all respects, and to have tractions specified over the portion of the (external and internal) surfaces designated by S_T and displacements specified over the remaining surfaces S_U ; the complete boundary is designated by S . Mixed conditions (e.g. normal displacement and shear traction) along a boundary may be specified; but for notational simplicity this situation is not explicitly stated in CP-III. All stresses σ_{ij} and displacements u_j in the viscoelastic problem, and σ_{ij}^R and u_j^R in the elastic problem (where $i, j = 1, 2, 3$) are referred to an orthogonal set of Cartesian coordinates x_i of the undeformed bodies. The n_i are components of the outer unit normal at any

point on the undeformed surface.

The braces $\{ \}$ denote a convolution integral,

$$\{Edf\} \equiv E_R^{-1} \int_{-\infty}^t E(t - \tau) \frac{\partial f}{\partial \tau} d\tau \quad (3)$$

where f is a function of time such as σ_{ij} or σ_{ij}^R , E_R is an arbitrarily selected constant (usually with units of modulus) and $E(t)$ is the uniaxial, linear viscoelastic relaxation modulus; for an elastic material, E is the Young's modulus. In many cases the quantity $\{Ddf\}$ will be used; it is defined using the creep compliance $D(t)$,

$$\{Ddf\} \equiv E_R \int_{-\infty}^t D(t - \tau) \frac{\partial f}{\partial \tau} d\tau \quad (4)$$

where $D(t)$ and $E(t)$ are interrelated according to

$$\int_0^t E(t - \tau) \frac{dD}{d\tau} d\tau = \int_0^t D(t - \tau) \frac{dE}{d\tau} d\tau = 1 \quad (5)$$

for $t > 0$; also $E = D = 0$ for $t < 0$. The lower limit is to be interpreted as 0^- in order to include the singularity in the derivatives at $\tau=0$.

Additional relationships which will be needed later, and which follow directly from (3) - (5), are concerned with inverses of the linear operators denoted by the braces. Namely, if

$$g = \{Ddf\} \quad (6)$$

then

$$f = \{Edg\} \quad (7)$$

or, equivalently,

$$f = \{Ed\{Ddf\}\} \quad (8)$$

and

$$f = \{Dd\{Edf\}\} \quad (9)$$

Equations (8) and (9) may be easily verified by Laplace transforming them and then using the Laplace transform of (5); the two-sided Laplace transform can be used in the event that f and g do not vanish at negative times.

In the earlier work [26] we assumed that all stresses and strains vanish for $t < 0$, while here this assumption is not made. One can, of course, always use a lower limit of zero in (3) and (4) by shifting the time axis so that the body is unstressed and unstrained for $t < 0$. However, when using CP-III in problems for which $dS_T/dt > 0$ (such as crack growth) before $dS_T/dt < 0$ (such as crack healing) it may be helpful to select $t=0$ to follow the $dS_T/dt > 0$ process; with this convention stresses and strains may exist at $t=0$ without invalidating CP-III if they can be calculated without regard to the $dS_T/dt > 0$ process. Such a situation arises if a crack first grows and then is arrested for a long enough time that the mechanical state of the continuum at $t=0$ is the same as if the crack's geometry had not changed when $t < 0$. Consequently, one can solve the crack shortening problem for $t \geq 0$ by assuming there is no change in crack dimensions for $t < 0$.

Returning to CP-III, the elastic problem is defined by the standard equilibrium equations with a body force F_i^R ,

$$\partial \sigma_{ij}^R / \partial x_j + F_i^R = 0, \quad (10)$$

strain-displacement equations,

$$\epsilon_{ij}^R = \frac{1}{2}(\partial u_i^R / \partial x_j + \partial u_j^R / \partial x_i) \quad (11)$$

and stress-strain equations,

$$\epsilon_{ij}^R = [(1 + \nu)\sigma_{ij}^R - \nu\delta_{ij}\sigma_{kk}^R]/E_R \quad (12)$$

where $k = 1, 2, 3$. The usual summation convention is used in that summation over the range of the repeated index is implied. Also, E_R and ν are the Young's modulus and Poisson's ratio, respectively, for the elastic problem, and δ_{ij} is the Kronecker delta (i.e., $\delta_{ij} = 1$ if $i = j$ and $\delta_{ij} = 0$ if $i \neq j$). The boundary conditions are

$$\sigma_{ij}^R n_j = T_i^R \quad \text{on } S_T \quad (13)$$

$$u_i^R = U_i^R \quad \text{on } S_U \quad (14)$$

The quantities F_i^R and T_i^R specified in the elastic problem are not the same as the traction T_i and body force F_i specified in the viscoelastic problem of interest. Rather, they are to be found using the convolution integrals,

$$F_i^R = \{DdF_i\} \quad (15)$$

$$T_i^R = \{DdT_i\} \quad (16)$$

However, the specified displacements are the same for both problems,

$$u_i^R = U_i \quad (17)$$

The viscoelastic boundary value problem is defined by the field equations

$$\partial\sigma_{ij}/\partial x_j + F_i = 0, \quad \epsilon_{ij} = \frac{1}{2} (\partial u_i/\partial x_j + \partial u_j/\partial x_i) \quad (18)$$

$$\epsilon_{ij} = [(1 + \nu)\{Dd\sigma_{ij}\} - \nu\delta_{ij}\{Dd\sigma_{kk}\}]/E_R \quad (19)$$

and boundary conditions,

$$\sigma_{ij} n_j = T_i \quad \text{on } S_T \quad (20)$$

$$u_i = U_i \text{ on } S_u \quad (21)$$

Observe that (19) is the constitutive equation for a viscoelastic material with a constant Poisson's ratio. The factor E_R^{-1} is introduced to cancel the factor E_R in the definition of $\{ \}$ in (4).

That the viscoelastic solution obtained using CP-III, (1) and (2), satisfies the governing equations (18) - (21) may be shown by substituting it into these equations, and then employing (6) - (9) and the fact that the elastic solution satisfies (10) - (17) and that $\partial n_i / \partial t = 0$ on S_T ; the last condition excludes rotation of the normal on S_T surfaces which, for example, could arise from melting or ablation. It should be noted that the traction T_i^R , (16), in the elastic problem is in general different from that in the viscoelastic problem. However, the condition $dS_T/dt < 0$ stated in CP-III implies the latter is known at all past times and thus T_i^R may be explicitly calculated.

When considering the problem of bonding of two different materials, a complication arises because the interfacial stresses acting across the bonding surface are not necessarily equal in the elastic problem. With reference to Fig. 2, let us use superscripts (+) and (-) to denote quantities above and below the surface $y=0$, respectively. For the viscoelastic problem $T_i^+ + T_i^- = 0$ along this surface, whereas from (16) the elastic traction sum is

$$\begin{aligned} T_i^{R+} + T_i^{R-} &= \{D^+ dT_i^+\} + \{D^- dT_i^-\} \\ &= \{(D^+ - D^-)dT_i^+\} \end{aligned} \quad (22)$$

If

$$E_R^+ D^+ = E_R^- D^- \quad (23)$$

then $T_i^{R+} + T_i^{R-} = 0$ or, equivalently, the interfacial elastic stress above the

bonding surface equals those below it. If D^- is proportional to D^+ we can select E_R^-/E_R^+ so that the traction sum in (22) vanishes. When the materials are not the same and the Poisson's ratios are not one-half, normal surface tractions induce material-dependent shear tractions (unless the friction coefficient vanishes) and thus a pure mode I state does not exist at the tip [27].

In order to avoid mathematical complexities that would make it difficult to understand the basic physics of the viscoelastic bonding problem, we shall assume that if bonding is not between bodies of the same material then, at least, their Poisson's ratios are one-half and their creep compliances are proportional, (23). If one body is much stiffer than the other, so that its deformation can be neglected, clearly we may use the results from an analysis based on these conditions even if the relatively rigid body does not satisfy them.

4. Results from crack-tip analysis

The opening displacement v above the bond surface in the neighborhood of the crack tip, Fig. 2, may be obtained from CP-III and the elastic solution in [4-I],

$$v = C_R \int_0^B \sigma_b^R(\xi') F(\xi'/\xi) d\xi' \quad (24)$$

where

$$F(\xi'/\xi) \equiv \frac{2}{\pi} [2(\xi/\xi')^{1/2} - \ln \left| \frac{1 + (\xi'/\xi)^{1/2}}{1 - (\xi'/\xi)^{1/2}} \right|] \quad (25)$$

and

$$C_R \equiv (1 - \nu^2)/E_R \quad (26)$$

The surface normal stress σ_b may be treated as a specified quantity, and therefore its counterpart σ_b^R in the elastic problem is obtained from (16),

which yields,

$$\sigma_b^R = \{Dd\sigma_b\} = E_R \int_{-\infty}^t D(t-\tau) \frac{\partial \sigma_b}{\partial \tau} d\tau \quad (27)$$

The superscript(+) is omitted until needed later to distinguish between quantities above and below the bond surface.

The stress singularity at the crack tip or bond edge is removed by using the Barenblatt result for elastic media [4],

$$K_I^R = \left(\frac{2}{\pi}\right)^{1/2} \int_0^\beta \sigma_b^R(\xi) \xi^{-1/2} d\xi \quad (28)$$

where K_I^R is the stress intensity factor for an elastic material with Young's modulus E_R and Poisson's ratio ν . This stress intensity factor is found from an elastic analysis for which $\sigma_b^R \equiv 0$, and is considered to be a known function of time in the present analysis. Equation (28) implies that β and/or σ_b^R must change with K_I^R if the stress at the crack tip is to be finite.

5. Prediction of quasi steady-state bonding speed when σ_b is constant

Equations (24) - (28) will be used along with an energy criterion for bonding to predict β and bonding speed $\dot{a}_b (= -\dot{a})$ as functions of K_I^R . It is assumed that σ_b is independent of time and is spatially uniform over $0 < \xi < \beta$. Also, \dot{a}_b is assumed to be essentially independent of time during the time it takes for the tip P to move the distance β ; \dot{a}_b may vary appreciably with time over propagation distances which are large compared to β , and thus the terminology quasi steady-state bonding is used. In the Appendix a formulation involving a spatially varying σ_b is analyzed, as mentioned previously.

Consider now the process of bonding, $\dot{a} > 0$, and identify in Fig. 2 a material particle ($x = \text{constant}$, $y = 0$) which is currently on the unloaded surface, $\xi > \beta$. Suppose at time $t=t_1$ the left end of the bonding zone,

$\xi=\beta$, arrives. This particle is acted on by the constant σ_b until $t=t_2$ when the right end of the zone, $\xi=0$, arrives. The work per unit surface area done on the particle by σ_b is $\sigma_b v_b$, where v_b is v at $\xi=\beta$, assuming that $v=0$ at $\xi=0$. The lower material may not be the same as the upper material and therefore the displacements may be different. This difference will be identified later; but, for now, we shall consider only the displacement above the bond plane.

The problem at hand is to use (24)-(28) to obtain v_b and thus $\sigma_b v_b$. By adding this work to that for the lower surface and equating the result to the so-called bond energy denoted by $2r_b$ (per unit area) an equation for predicting \dot{a}_b is obtained. First we need σ_b^R , which may be found from (27) by noting that $\sigma_b = 0$ for $t < t_1$ and σ_b is constant for $t_1 < t < t_2$; thus, for a particle at fixed x and with $t_1 < t < t_2$,

$$\sigma_b^R = E_R \sigma_b D(t-t_1) \quad (29)$$

The relationship between t and ξ follows from the quasi steady-state assumption,

$$\xi = (t_2 - t)\dot{a}_b \quad \text{and} \quad \beta = (t_2 - t_1)\dot{a}_b \quad (30)$$

from which

$$t - t_1 = (\beta - \xi)/\dot{a}_b \quad (31)$$

Generalized power law creep compliance

The creep compliance of many materials can be well-represented over several decades of time by the so-called generalized power law,

$$D(t) = D_0 + D_1 t^m \quad (32)$$

where D_0 , D_1 and m are positive constants and $0 < m \leq 1$. We shall use this form to obtain exact results and then, guided by these findings, develop an

approximate formula for more general forms of creep compliance. From (29), (31), and (32),

$$\sigma_b^R = E_R \sigma_b [D_0 + D_1 (1-\eta)^m (\beta/\dot{a}_b)^m] \quad (33)$$

where

$$\eta \equiv \xi/\beta \quad (34)$$

Substitute (33) into (28) and find

$$K_I^R = (8/\pi)^{1/2} E_R \sigma_b \beta^{1/2} [D_0 + D_1 \gamma_m (\beta/\dot{a}_b)^m] \quad (35)$$

where

$$\gamma_m \equiv (\pi/4)^{1/2} \Gamma(1+m)/\Gamma(1.5+m) \quad (36)$$

and $\Gamma(\cdot)$ is the Gamma function. Observe that the relationship between β and K_I^R depends on bonding speed, whereas the analogous relationship for crack growth (which relates "failure zone" or "fracture process zone" length a to K_I) does not depend explicitly on speed [4-I]. Next, use (33) in (24) to find the displacement at $\xi=\beta$, and thus the work $\sigma_b v_b$. It is helpful to integrate-by-parts the term involving the logarithm and obtain, finally,

$$W_b \equiv \sigma_b v_b = \frac{4}{\pi} (1-\nu^2) \sigma_b^2 \beta [D_0 + D_1 c_m \gamma_m (\beta/\dot{a}_b)^m] \quad (37)$$

where

$$c_m \equiv (2m+1)/(m+1) \quad (38)$$

Previously we introduced superscripts (+) and (-) to denote quantities above and below the bond plane. In view of (23),

$$E_R^+ D_0^+ = E_R^- D_0^- \quad \text{and} \quad E_R^+ D_1^+ = E_R^- D_1^- \quad (39)$$

Recall that the Poisson's ratios are assumed equal and constant. The superscripts can be omitted in (35) as only these products appear. However,

the work above the bond plane, which will now be denoted by w_b^+ , may be different from that below, w_b^- , since E_R does not appear as a factor. Indeed, from (37),

$$w_b^- / w_b^+ = D_0^- / D_0^+ = D_1^- / D_1^+ \quad (40)$$

The criterion for bonding may be written as

$$2r_b = w_b^+ + w_b^- = (1 + D_0^- / D_0^+) w_b^+ \quad (41)$$

or, equivalently,

$$2r_b' = w_b^+ \quad (42)$$

where

$$r_b' \equiv r_b / (1 + D_0^- / D_0^+) \quad (43)$$

For identical materials (42) reduces to $r_b = w_b^+$, whereas if the lower material is rigid, $2r_b = w_b^+$. We shall use the effective bond energy r_b' in all subsequent work so that the notation in the results does not have to be changed when considering the bonding of materials with the same or different stiffnesses; the effect of the lower material will appear only in (43) until we apply the theory in Section 7.

Equations (35) and (42), where (37) is used for w_b^+ , may be solved to obtain β and \dot{a}_b in terms of K_I^R , given σ_b and r_b' . We assume these latter two quantities are constants and obtain, finally,

$$\beta / \beta_m = Z(1+\lambda)^{-2} c_m^2 \quad (44)$$

where

$$\beta_m \equiv \pi r_b' / 2 \sigma_b^2 (1-\nu^2) D_0^+ c_m^2 \quad (45)$$

is a constant with the dimension of length. Also,

$$\dot{a}_b/\dot{a}_m = Z(1+\lambda)^{-2} \lambda^{-(1/m)} c_m^{(2+1/m)} \quad (46)$$

where

$$\dot{a}_m \equiv \beta_m (D_{1\gamma_m}/D_{0c_m})^{1/m} \quad (47)$$

is a constant with dimensions of velocity. The quantity λ is a function of Z , as found from the solution to a quadratic equation,

$$\lambda = 0.5[c_m Z + (c_m Z)^{1/2}(c_m Z + 4/c_m - 4)^{1/2}] - 1 \quad (48)$$

In turn,

$$Z \equiv (K_I^R/K_{I0}^R)^2 \quad (49)$$

where

$$(K_{I0}^R)^2 \equiv 4\tau_b^+ D_0^+ (E_R^+)^2/(1-\nu^2) \quad (50)$$

is a constant with dimensions of stress intensity factor squared.

For the range $1 < Z < \infty$, we find both β and \dot{a}_b are monotone decreasing functions of Z and that

$$\lambda \rightarrow 0 \text{ as } Z \rightarrow 1 \text{ and } \lambda \approx c_m Z \text{ for } Z \gg 1 \quad (51)$$

This behavior yields from (44),

$$\beta/\beta_m \rightarrow c_m^2 \text{ as } Z \rightarrow 1 \text{ and } \beta/\beta_m \approx Z^{-1} \text{ for } Z \gg 1 \quad (52)$$

and from (46),

$$\dot{a}_b/\dot{a}_m \rightarrow \infty \text{ as } Z \rightarrow 1 \text{ and } \dot{a}_b/\dot{a}_m \approx Z^{-(1+1/m)} \text{ for } Z \gg 1 \quad (53)$$

Figures 3 and 4 show the normalized bonding-zone length (44) and bonding speed (46) as functions of Z on logarithmic scales ($\log \equiv \log_{10}$). The range of values c_m and Z for which the behavior is essentially that for the high stress intensity factor range in (52) and (53) may be seen. In this range the

results are the same as the exact solution over $0 < K_I^R < \infty$ for a pure power-law material, (32) with $D_0 = 0$.

In order to obtain explicit analytical results for $Z \gg 1$, β_m and \dot{a}_m may be substituted into (44) and (46) in order to eliminate D_0 . The results for $Z \gg 1$ are

$$\beta = 2\pi [\gamma_b' E_R^+ / (1-\nu^2) \sigma_b c_m K_I^R]^2 \quad (54)$$

$$\dot{a}_b = \pi [4\gamma_b']^{(2+1/m)} [(1-\nu^2) E_R^+ \gamma_m / c_m]^{1/m} [E_R^+ / (1-\nu^2) K_I^R]^{2(1+1/m)} / 8\sigma_b^2 c_m^2 \quad (55)$$

These forms, i.e.,

$$\beta = k_1 (K_I^R / E_R^+)^{-2}, \quad \dot{a}_b = k (K_I^R / E_R^+)^{-q}, \quad q \equiv 2(1+1/m) \quad (56)$$

(where k_1 and k are positive constants) are like those for the crack growth problem; but the exponents on stress intensity factor in the fracture problem are positive. Here, both the bonding-zone length and speed increase with decreasing K_I^R . Immediate bonding occurs when $K_I^R = K_{I0}^R$ since $\dot{a}_b = \infty$ at this limit; the corresponding value for β is $\beta_m c_m^2$, (52).

For $K_I^R < K_{I0}^R$, (48) yields the result $\lambda < 0$. A physical interpretation of this low K_I^R behavior may be made by noting that for $K_I^R > K_{I0}^R$, \dot{a}_b increases with increasing effective bond energy γ_b' , for K_I^R fixed (cf. (45)-(50)). When $K_I^R < K_{I0}^R$ there is more work available than required to draw the surfaces together, neglecting the effects of material inertia. Hence, for $K_I^R \leq K_{I0}^R$ a dynamic analysis would be needed to predict finite, high speed bonding.

General creep compliance

The foregoing results based on the generalized power law compliance (32) are helpful in extending the theory to a more general creep compliance, which we write in the form

$$D(t) = D_0 + \Delta D(t) \quad (57)$$

where D_0 , as before, is the initial compliance; thus, $\Delta D(0^+) = 0$. This compliance and (29) - (31) yield

$$\sigma_b^R = \sigma_b^R(\xi) = E_R \sigma_b \{D_0 + \Delta D[(\beta - \xi)/\dot{a}_b]\} \quad (58)$$

This function is to be used in (28), which will be evaluated approximately using a method like that used in crack growth analyses [4-II]. First, rewrite (28) by introducing a logarithmic transformation to change the integration variable to L ,

$$L \equiv \log(1 - r) \quad (59)$$

where, as before, $\log \equiv \log_{10}$ and $r = \xi/\beta$. Equation (28) becomes

$$K_I^R = \left(\frac{2}{\pi}\right)^{1/2} (\ln 10)^{1/2} \int_{-\infty}^0 \sigma_b^R w_1 dL \quad (60)$$

where

$$w_1 \equiv (1 - 10^L)^{-1/2} 10^L \quad (61)$$

is a weight function; it is drawn in Fig. 5. Because this function is very small except for L close to zero (corresponding to $\xi=0$), and ΔD in (58) decreases with decreasing L (or increasing ξ), only the behavior of $\Delta D(t)$ for $t \approx \beta/\dot{a}_b$ needs to be considered (cf. (58)). Let us assume that ΔD may be approximated by a power law $\Delta D = D_1 t^m$ over at least a one-decade time range (say), i.e. $\beta/10\dot{a}_b \leq t \leq \beta/\dot{a}_b$ (which corresponds to $-1 \leq L \leq 0$) and that behavior for smaller times is unimportant because w_1 is so small when $L < -1$, (35) may be used, in which

$$m \equiv \frac{d \log \Delta D}{d \log t} \quad (62)$$

where $t = \beta/\dot{a}_b$. A more compact way of writing (35) is

$$\kappa_I^R = \left(\frac{8}{\pi}\right)^{1/2} E_R \sigma_b \beta^{1/2} D(t') \quad (63)$$

where

$$t' \equiv \gamma_m^{1/m} \beta/\dot{a}_b \quad (64)$$

It is found that $\gamma_m^{1/m}$ is practically constant; this factor is a monotone increasing function of m , in which $0.541 < \gamma_m^{1/m} \leq 2/3$ for $0 \leq m \leq 1$.

The displacement (24) is needed to obtain the work $W_b = \sigma_b v_b$, where $v_b \equiv v$ at $\xi = \beta$. Using (59) we find

$$v_b = \frac{4}{\pi} C_R \beta (\ln 10) \int_{-\beta}^0 \sigma_b^R w_2 dL \quad (65)$$

where

$$w_2 \equiv 0.5 \left| 2r^{-1/2} - \ln \left| \frac{1+\eta}{1-\eta} \right| \right| 10^L \quad (66)$$

and $r = 1-10^L$. The graph of the weight function w_2 in Fig. 5 shows that, just as for w_1 , the behavior of σ_b^R (and thus ΔD) is relatively unimportant for $L < -1$. Just as (35) has been replaced by (63), we may replace (37) by

$$W_b = \frac{4}{\pi} (1-v^2) \sigma_b^2 \beta D(t'') \quad (67)$$

where

$$t'' \equiv \gamma_m^{1/m} \beta/\dot{a}_b \quad (68)$$

and

$$\gamma_m' \equiv C_m \gamma_m \quad (69)$$

The factor $\gamma_m^{1/m}$ is a monotone decreasing function of m , in which $1 \geq \gamma_m^{1/m} < 1.47$ for $1 \geq m \geq 0$.

The bonding criterion (42) may now be written as

$$2\tau_b' = \frac{4}{\pi} (1-v^2) \sigma_b^2 \beta D^+(t'') \quad (70)$$

which together with (63) (recalling that $E_R D = E_R^+ D^+$) provides the pair of equations for finding β and \dot{a}_b . The previous results, (44) and (46), could be used as first approximations in an iterative solution approach. Here, we shall discuss only the low and high speed limiting conditions for bonding.

Previously, it was found that β and \dot{a}_b are monotone decreasing functions of K_I^R , for $K_I^R > K_{I0}^R$. However, \dot{a}_b may vanish at a finite value of K_I^R , as will be shown by using (70) together with (54) for β . Although the latter equation is exact only for a pure power law compliance, it is expected to be a good approximation whenever the compliance can be approximated by a power law over one-decade time intervals. (Observe that β depends on m through c_m , (38), but not on D_1 ; m is now given by (62).) Substitute (54) for β into (70) and obtain

$$(K_I^R)^2 = 4 \pi_b^2 D^+(t'') (E_R^+)^2 / (1-\nu^2) c_m^2 \quad (71)$$

where t'' is in (68). With increasing K_I^R , $D^+(t'')$ must increase according to (71). However, if the creep compliance has a finite upper limiting value D_∞^+ , i.e. $D_\infty^+ \equiv D^+(\infty) < \infty$, then the largest value of K_I^R for which a solution \dot{a}_b exists is $K_{I\infty}^R$, where

$$(K_{I\infty}^R)^2 = 4 \pi_b^2 D_\infty^+ (E_R^+)^2 / (1-\nu^2) \quad (72)$$

When $t'' \rightarrow \infty$, then $D^+ \rightarrow D_\infty^+$, and the slope m vanishes; thus $c_m \rightarrow 1$ as $t'' \rightarrow \infty$.

A further study of (71), in which it is assumed that m in (62) does not increase with t , along with the previous results (44) and (46), leads to the following inequalities and behavior. For $K_{I0}^R < K_I^R < K_{I\infty}^R$, the length β and speed \dot{a}_b are monotone decreasing functions of K_I^R ; also,

$$\beta \rightarrow \beta_m c_m^2 \quad \text{and} \quad \dot{a}_b \rightarrow \infty \quad \text{as} \quad K_I^R \rightarrow K_{I0}^R \quad (73)$$

$$\beta \rightarrow \beta_m c_m^2 D_0/D_\infty \quad \text{and} \quad \dot{a}_b \rightarrow 0 \quad \text{as} \quad K_I^R \rightarrow K_{I\infty}^R \quad (74)$$

Recall that D_0/D_∞ above the bond surface is the same as that below. From (50) and (72),

$$K_{I\infty}^R/K_{I0}^R = (D_\infty/D_0)^{1/2} \quad (75)$$

6. Comparison of apparent fracture and bond energies

In many situations involving slow loading or unloading of rubber, the global behavior is elastic, with this behavior defined in terms of elastic constants which are essentially equal to the long-time values of the associated viscoelastic properties. On the other hand, at this same time viscoelastic effects may be very pronounced in the neighborhood of a moving crack tip or contact edge because of the high local strain rates.

This situation is easily represented in the theory at hand by taking as the arbitrary reference elastic modulus the reciprocal of the actual long-time compliance; thus $D_\infty^+ = 1/E_R^+$ and $D_\infty^- = 1/E_R^-$. With this global elastic behavior, it is common practice to define an apparent fracture energy associated with crack growth by means of an elastic-like equation for fracture; in terms of the notation and theory at hand, in which adhesive and cohesive fracture are considered,

$$r'_{af} \equiv (1-\nu^2) D_\infty^+ K_I^2/4 \quad (76)$$

where K_I is the stress intensity factor which produces a particular crack speed, \dot{a} . Similarly, guided by (72), we may define a apparent bond energy using the same expression,

$$r'_{ab} \equiv (1-\nu^2) D_\infty^+ (K_I^R)^2/4 \quad (77)$$

where K_I^R produces a bonding rate \dot{a}_b ; since the actual global behavior is also that of the reference elastic problem, $K_I = K_I^R$.

The apparent energies in (76) and (77) can be related to the (intrinsic) effective fracture energy Γ_f' and bond energy Γ_b' . From [4-II], after allowing for adhesive fracture through an equation analogous to (43),

$$\Gamma_f' = (1-\nu^2)D^+(\alpha/3\bar{a})K_I^2/4 \quad (78)$$

and by eliminating K_I^2 between (76) and (78) we find

$$\Gamma_{af}' = \Gamma_f' D_\infty/D(\alpha/3\bar{a}) \quad (79)$$

The compliance ratio is the same above and below the bond surface, as assumed previously. Similarly, from (71) and (77),

$$\Gamma_{ab}' = \Gamma_b' D(t'')/D_\infty c_m^2 \quad (80)$$

The ratio $D_\infty/D(t)$ increases monotonically (from unity) as time t decreases from infinity to zero, and for rubber D_∞/D_0 may exceed one hundred [28]. Hence, the ratios Γ_{af}'/Γ_f' and Γ_b'/Γ_{ab}' may themselves exceed one hundred. Moreover, if the effective energies are equal, $\Gamma_f' = \Gamma_b'$, the ratio of apparent energies is bounded according to

$$1 \leq \frac{\Gamma_{af}'}{\Gamma_{ab}'} \leq (c_m D_\infty/D_0)^2 \quad (81)$$

In experiments on the time-dependent adhesion of rubber to glass, Roberts and Thomas [11] found that the ratio $\Gamma_{af}'/\Gamma_{ab}'$ is indeed very large over a wide range of bonding and debonding speeds. This ratio was reported to exceed one thousand at the shortest testing time, which was approximately ten seconds.

Finally, it is of interest to observe for this case of global elastic behavior that (72) reduces to

$$K_{I\infty}^2 = 4\Gamma_b'/D_\infty^+(1-\nu^2) \quad (82)$$

and that $\dot{a}_b > 0$ if $K_I < K_{I\infty}$. For the fracture problem $\dot{a} > 0$ if $K_I > K_{I\infty}^f$, where

$$(K_{I\infty}^f)^2 \equiv 4\Gamma_f^*/D_\infty^+(1-\nu^2) \quad (83)$$

Consequently, if the bond and fracture energies are equal, (82) or (83) define a value of the stress intensity factor below which there is bonding and above which there is crack growth.

7. Examples

Cohesive crack healing

Consider the Griffith type of problem in which there is an isolated circular crack with radius a , or a through-the-thickness crack of length $2a$. A remote, uniform tensile stress $\sigma(t)$ normal to the crack plane is given. In the reference elastic body the stress intensity factor is [29],

$$K_I^R = c a^{1/2} \sigma^R \quad (84)$$

where c is a constant; $c = 2/\pi^{1/2}$ for a circular crack and $c = \pi^{1/2}$ for a through-crack. Equation (16) or the inverse of (1) provides σ^R ,

$$\sigma^R = E_R \int_{-\infty}^t D(t-\tau) \frac{d\sigma}{d\tau} d\tau \quad (85)$$

which is assumed to be non-negative for (84) to be valid. Let us use the power law in (56) for \dot{a}_b ; then with (84) for K_I^R and with $\dot{a}_b = -\dot{a}$, we find

$$a/a_0 = (1-I_t)^{1/p} \quad (86)$$

where a_0 is the size at $t=0$. Also,

$$p \equiv q/2 + 1 = (1+2m)/m \quad (87)$$

$$I_t = k_2 p a_0^{-p} \int_0^t (c \sigma^R / E_R)^{-q} dt \quad (88)$$

The healing time t_h is defined as the time at which $a=0$; namely, $I_t(t_h) = 1$. An explicit solution for t_h may be easily found if σ is a constant which is applied long before $t=0$, so that (85) yields $\sigma^R = E_R D_\infty \sigma$, where $D_\infty \equiv D(\infty)$ is the equilibrium or long-time creep compliance. Equation (88) reduces to

$$I_t = k_2 p a_0^{-p} (c D_\infty \sigma)^{-q} t \quad (89)$$

and thus

$$t_h = a_0^p (c D_\infty \sigma)^q / k_2 p \quad (90)$$

Observe that, as expected, the higher the tensile stress σ , the longer the healing time. Also, notice that the arbitrary constant E_R does not appear in the prediction of a and t_h because σ^R / E_R is independent of E_R (cf. (85)).

It should be recalled that whether or not healing or crack growth occurs depends on the value of K_I^R relative to $K_{I\infty}^R$ in (72). For the cohesive healing problem, $r_b' = r_b/2$ and $D_\infty^+ = D_\infty$. Using also (84) and (85) the criterion for bond growth is found as

$$c a^{1/2} \int_{-\infty}^t D(t-\tau) \frac{d\sigma}{d\tau} d\tau < [2 r_b D_\infty / (1-\nu^2)]^{1/2} \quad (91)$$

For a pure power law compliance (which includes that for a Newtonian body, $m=1$) $D_\infty = \infty$, and (91) is always satisfied if $(\sigma, t) < \infty$. But crack growth analysis shows that the criterion for growth also is always satisfied [4-II]. This quasi-steady state analysis is thus not sufficient to determine the sign of \dot{a} for a power law material.

Growth of contact area between initially curved surfaces

Figure 6 shows the contact region for two bodies which are pressed together by the load F and are also drawn together under bonding stress σ_b .

The length scale β over which σ_b acts is assumed to be very small compared to the contact size. Just as in the fracture problem (i.e. contact area reduction) the opening displacement is parabolic near the contact edge except very close to the edge where the cusp shape of Fig. 2 exists, shown in Fig. 6 by the blackened edge area. In order to predict $\dot{a}_b (= \dot{a}_c)$ the stress intensity factor for the reference elastic problem K_I^R is needed. Here, we shall consider two cases: (i) contact between initially spherical surfaces with radii R^+ and R^- and (ii) the same type of problem, except the surfaces are cylindrical so that the deformation is two-dimensional. An approach to finding K_I^R will be used which is similar to that in [12] for contact between a plane and a spherical surface.

First, in the absence σ_b , Hertz's solutions for contact size may be used for the spherical surfaces,

$$a_c^3 = 3F_H^R / 8BE_R' \quad (92)$$

and the cylindrical surfaces,

$$a_c^2 = 2F_H^R / \pi BE_R' \quad (93)$$

where F_H^R in (92) is the total force, while in (93) it is force per unit length along the cylinder axis. Also,

$$B \equiv (1/R^+ + 1/R^-)/2, \quad \frac{1}{E_R'} \equiv \left(\frac{1}{E_R^+} + \frac{1}{E_R^-} \right) (1-\nu^2) \quad (94)$$

Now, let us reduce the compressive load by an amount ΔF^R ; assume the surfaces are bonded so that a_c is fixed at the Hertz value. This change produces an interface tensile stress which is infinite at the contact edges (without the Barenblatt modification), because these edges are really crack tips. The stress intensity factor may be obtained from the solution for the

normal stress between a bonded flat-ended rigid punch under tensile load ΔF^R and flat elastic halfspace [25], using the assumption that $a_c \ll R^+$ and $a_c \ll R^-$; the Hertz solutions, (92) and (93), are based on this assumption, which we retain. That this is the same normal stress as produced by ΔF^R in the problem in Fig. 6 may be argued by first noting that it is independent of elastic constants and the initial surface radii, and produces a rigid translation of the contact surface. The same normal stress acts on both upper and lower surfaces, and since the contact surface shape does not change the upper and lower bodies remain in contact. Because the interface conditions are satisfied using this normal stress and the bodies are, in-effect, halfspaces (i.e. $a_c \ll R^+$ and $a_c \ll R^-$), it is the one and only solution for interface stress. (However, the conditions for zero interfacial shear stress must be met, as discussed at the end of Section 3.)

For a circular punch with radius a_c , the contact stress is,

$$\begin{aligned} \sigma_y^R &= \frac{\Delta F^R}{2\pi a_c (a_c^2 - r^2)^{1/2}} \\ &= \frac{\Delta F^R}{2\pi a_c (a_c + r)^{1/2} (a_c - r)^{1/2}} \end{aligned} \quad (95)$$

where r is the radial distance from the contact center to a point on the interface. From the singularity at $r=a_c$ and the definition of stress intensity factor,

$$K_I^R = \lim_{r \rightarrow a_c} [2\pi(a_c - r)]^{1/2} \sigma_y^R \quad (96)$$

we obtain

$$K_I^R = \Delta F^R / 2\pi^{1/2} a_c^{3/2} \quad (97)$$

Similarly, for the plane strain problem,

$$K_I^R = \Delta F^R / (\pi a_c)^{1/2} \quad (98)$$

Now, $\Delta F^R = F_H^R - F^R$, where F^R is the total load. With this expression and F_H^R from (92) and (93), the stress intensity factor in (97) for spherical surfaces becomes,

$$K_I^R = 4BE_R' a_c^{3/2} / 3\pi^{1/2} - a_c^{-3/2} F^R / 2\pi^{1/2} \quad (99)$$

For cylindrical surfaces,

$$K_I^R = \pi^{1/2} BE_R' a_c^{3/2} / 2 - a_c^{-1/2} F^R / \pi^{1/2} \quad (100)$$

The force F^R in the elastic problem is related to the actual compressive force through $F^R = \{DdF\}$, just as the stress in (85). Introduction of K_I^R in terms of a_c makes (99) and (100) differential equations for a_c .

As simple examples, the contact size will be found analytically from these differential equations using the power law bonding speed equation (56) for two cases: $F^R = 0$ and $K_I^R = 0$. In the first case, (99) yields the radius

$$a_c = A t_b^s \quad (101)$$

where t_b is the bonding time, and

$$s \equiv 2/(3q+2) \quad (102)$$

Also

$$A \equiv [k(3\pi^{1/2} D' / 4B)^q / s]^s \quad (103)$$

$$D' \equiv (1 + D_1^- / D_1^+)(1 - \nu^2) \quad (104)$$

The last equality comes from (39). In deriving (101) we assumed interfacial contact starts at $t=0$ and neglected the error in the Barenblatt method at short times (when $a_c < \delta$). The size a_c for contact between cylinders has the

same time dependence as in (101) because (100) depends on a_c in the same way as (99) when $F^R = 0$. From (56) and (102),

$$s = m/(3+4m) \quad (105)$$

If $m=1$ (viscous material) then $s=1/7$, which is the largest physically acceptable exponent.

The time dependence of a_c in (101) is in general considerably different from that predicted from the Hertz contact problem. Taking for example a constant load F applied at $t=0$, the load in the elastic problem is $F^R = E_R^+ D_1^+ t_b^m F$. From (99) and (100), respectively,

$$a_c = (3D_1^+ F/8B)^{1/3} t_b^{m/3} \quad (106)$$

$$a_c = (2D_1^+ F/\pi B)^{1/2} t_b^{m/2} \quad (107)$$

(Anand's model [13] predicts this time-dependence for a power law material.)

Now, let us retain K_I^R but assume it is small enough that a_c is close to the Hertz solutions (106) and (107). For the power law of (56), this occurs when \dot{a}_b is sufficiently large. Let a_H be the Hertz solution, which is for $K_I^R = 0$ in (99) and (100). Then $a_c = a_H + \Delta a$, where $\Delta a/a_H \ll 1$ by assumption. Using this approximation in (99) we find

$$\Delta a/a_H = \pi^{1/2} D_1^+ (k/\dot{a}_H)^{1/q} / 4Ba_H^{3/2} \quad (108)$$

where a_H is the solution to (99) for $K_I^R = 0$. For example, using (106), $\Delta a/a_H \sim t_b^{-2m^2/3(m+1)}$, and thus the error in the Hertz solution (106) diminishes with time. A similar result, with the same exponents as in (108), is found for the contact between cylinders; using (107), we find again that the error diminishes with time in that $\Delta a/a_H \sim t_b^{-m(1+4m)/4(1+m)}$.

Effect of bonding time on joint strength

As discussed in Section 1, the time-dependent strength of bonds formed across contacting surfaces has received considerable attention. The examples considered in the present section deal only with contact area growth and not the processes following contact, such as polymer-polymer interdiffusion (which may be very significant if the temperature is sufficiently high). Here, we observe only that (99) and (100) may be used to predict strength, if the residual viscoelastic effect of the bonding problem is negligible so that the correspondence principle for crack growth may be used. In this case, the elastic and viscoelastic stresses, loads, and stress intensity factors are the same. Suppose, for example, that following the bonding process the temperature is reduced enough that the critical stress intensity factor K_{IC} is a constant and that the first term in (99) is negligible at fracture. Then the strength is $F \sim a_c^{3/2} K_{IC}$. Using (101), $F \sim t_b^{3s/2}$, while from (106) $F \sim t_b^{m/2}$; for viscous media $m=1$, and the strengths are, respectively, $F \sim t_b^{.21}$ and $F \sim t_b^{.5}$.

If, following bonding, we use the idealization from [20] in which any nonuniformity in stresses in the bond is ignored, use elastic fracture mechanics, and assume the fracture energy γ_f' is proportional to bonded area A_b , then $K_{IC} \sim \gamma_f'^{1/2} \sim A_b^{1/2}$; with a given crack at the interface the joint strength is proportional to $A_b^{1/2}$. From (101), $K_{IC} \sim t_b^{s/2}$ for spheres and $K_{IC} \sim t_b^s$ for cylinders; if $m=1$, these exponents are 1/14 and 1/7, respectively. On the other hand from (106) and (107), $K_{IC} \sim t_b^{m/3}$ and $K_{IC} \sim t_b^{m/4}$, respectively.

For polymer-polymer bonding of noncrosslinked systems somewhat above the glass transition temperature, the behavior $K_{IC} \sim t_b^{1/4}$ is usually found experimentally [19,20] (in a range for which $m \approx 1$ is probably a good

assumption); it is also the behavior predicted from interdiffusion theory for fully contacted or wetted surfaces. None of the exponents discussed above yield the $1/4$ exponent (for the physically acceptable range of viscoelastic exponents $0 < m \leq 1$) except for the last one of $m/4$, if $m=1$, for contacting cylindrical surfaces. Anand [17] reported that when nearly flat surfaces are bonded, the initially irregular contacting areas become in time contacting cylinders, and that the conversion to cylindrical contact surfaces occurs early in the bonding process. For this case, one could not use an experimentally determined exponent of $1/4$ to conclude that the increase in joint strength is due to interdiffusion as opposed to contact growth. Of course, if the externally applied contact pressure is high enough during bonding so that essentially full contact is quickly established, contact area growth will not be an important source of time-dependence of the joint strength.

8. Conclusions

A mechanics-based theory of bonding between the same or different linear, isotropic viscoelastic media has been developed and used in some examples. We assumed quasi steady-state bonding and the bonding stress σ_b and energy Γ_b' to be independent of bonding speed \dot{a}_b in order to obtain explicit, closed-form solutions. However, if these material-related quantities vary with speed (which could be due to surface roughness on a scale which is very small compared to the bonding-zone length β) most of the equations do not have to be changed. For example, with speed dependence of these parameters, (55) becomes an implicit equation for \dot{a}_b ; with power law dependence, the resulting solutions for β and \dot{a}_b obey power laws in K_I^R , as in (56), but the exponents are in general different.

Regardless of how or if σ_b and r_b' depend on bonding speed, we may conclude that all dependence of \dot{a}_b and β on external loading and geometry of the continua is through the instantaneous stress intensity factor K_I^R . This simplicity exists as long as β is small compared to local geometric scales such as initial radii of surface asperities or crack length; as mentioned above, very small-scale roughness compared to β is also acceptable.

In contrast to the crack growth problem, K_I^R depends on external loading history, and \dot{a}_b and β decrease with increasing K_I^R . The external loading must be such that \dot{a}_b is nonnegative in order for the correspondence principle used in the analysis to be valid. The correspondence principles used for bond growth and crack growth are different. If crack healing occurs after crack growth, the bonding theory will not be valid unless effects of the prior history of crack growth have essentially faded out. The complexity of the analysis appears to be much greater when the velocity of the boundary of bonded surfaces changes sign and viscoelastic effects from before and after the change are combined; however, methods exist for analyzing this type of problem [30,31].

Linear theory may not be valid under high stresses, such as when bodies with initially curved surfaces are pressed together under high compressive loads. In such cases, a J integral theory may be applicable. It would be similar to that for crack growth, but based on correspondence principle III (instead of II, which is for crack growth) given in [26].

Although the development here is for isotropic media, through a change in the creep compliance $D(t)$ the theory in Sections 5 and 6 can be used for bonding of surfaces of orthotropic media if the surfaces and bond edge are parallel to principal material planes. This extension is based on the findings in [5] for crack growth, in which the equations for the mechanical

state near and at the interface are the same as for isotropic media; in this case $(1-\nu^2) D(t)$ is to be replaced by another function of time consisting of a combination of creep compliances of the orthotropic material. (The same generalization can be made in applications involving effectively unbounded media, such as those in Section 7.) However, just as for isotropic materials, property-dependent interfacial shear stresses develop unless the bonding is between the same materials or, if different, between incompressible materials with proportional compliances; one material may be rigid. The present theory has been developed under the condition that there is no shear stress at the interface in order to bring out the essential features of the mechanics of bonding or healing of viscoelastic materials with a minimum of mathematical complexity.

Finally, it should be noted that Poisson's ratio appears in elastic solutions in this paper only in the form $(1-\nu^2)/\text{modulus}$, as in (26) and (94). For problems in which this is the case, one can show by means of Graham's extended correspondence principle [6] that the theory remains valid when Poisson's ratio is time-dependent, as long as it is the same for the materials above and below the bond surface. In this situation one may use a plane-strain creep compliance $C(t)$ in place of $(1-\nu^2) D(t)$ throughout the paper; this replacement is analogous to the generalization made for orthotropic media, as discussed above.

Acknowledgement

Sponsorship of this research by the Office of Naval Research is gratefully acknowledged.

REFERENCES

- [1] M.L. Williams, in Proceedings 5th U.S. National Congress of Applied Mechanics, American Society of Mechanical Engineers (1966) 451-464.
- [2] M.L. Williams, International Journal of Fracture Mechanics 1 (1965) 292-310.
- [3] W.G. Knauss, in Deformation and Fracture of High Polymers, H. Henning Kausch, John A. Hassell and Robert I. Jaffee, Eds., Plenum Press (1974) 501-541.
- [4] R.A. Schapery, International Journal of Fracture 11 (1975): Part I, 141-159; Part II, 369-388; Part III, 549-562.
- [5] G.S. Brockway and R.A. Schapery, Engineering Fracture Mechanics 10 (1978) 453-468.
- [6] R.M. Christensen, Theory of Viscoelasticity, An Introduction, Second edn., Academic Press (1982).
- [7] J.G. Williams, Fracture Mechanics of Polymers, Halstead Press, John Wiley & Sons (1984).
- [8] R.A. Schapery, International Journal of Fracture 14 (1978) 293-309.
- [9] J.R. Walton, Journal of Applied Mechanics 54 (1987) 635-641.
- [10] K.L. Johnson, K. Kendall and A.D. Roberts, Proceedings of the Royal Society (London) A234 (1971) 301-313.
- [11] A.D. Roberts and A.G. Thomas, Wear 33 (1975) 45-64.
- [12] J.A. Greenwood and K.L. Johnson, Philosophical Magazine A 43 (1981) 697-711.
- [13] J.N. Anand and H.J. Karam, Journal of Adhesion 1 (1969) 16-23.
- [14] J.N. Anand and R.Z. Balwinski, Journal of Adhesion 1 (1969) 24-30.
- [15] J.N. Anand, Journal of Adhesion 1 (1969) 31-37.
- [16] J.N. Anand, and L. Dipzinski, Journal of Adhesion 2 (1970) 16-22.

- [17] J.N. Anand, Journal of Adhesion 2 (1970) 23-28.
- [18] J.N. Anand, Journal of Adhesion 5 (1973) 265-267.
- [19] H.H. Kausch, D. Petrovska, R.F. Landel and L. Monnerie, Polymer Engineering and Science 27 (1987) 149-154.
- [20] K. Jud, H.H. Kausch and J.G. Williams, Journal of Materials Science 16 (1981) 204-210.
- [21] R.G. Stacer and H.L. Schreuder-Stacer, International Journal of Fracture (in press).
- [22] J.W. Button, D.N. Little, Y. Kim and J. Ahmed, Proceedings Association of Asphalt Paving Technologists 5b (1987) 62-90.
- [23] A.H. Lepie, Proceedings JANNAF Structures and Mechanical Behavior Working Group CPIA Publication No. 351 (1981) 235-240.
- [24] R.A. Schapery, Tire Science & Technology 6 (1978) 3-47.
- [25] S.P. Timoshenko and J.N. Goodier, Theory of Elasticity, Third edn. McGraw-Hill (1970).
- [26] R.A. Schapery, International Journal of Fracture 25 (1984) 195-223.
- [27] M.A. Biot, Quarterly Applied Mathematics XXX (1972) 379-406.
- [28] J.D. Ferry, Viscoelastic Properties of Polymers, Third edn. Wiley (1980).
- [29] D. Broek, Elementary Engineering Fracture Mechanics, Fourth edn. Martinus Nijhoff (1986).
- [30] T.C.T. Ting, Journal of Applied Mechanics 33 (1966) 845-854.
- [31] G.A.C. Graham, International Journal of Engineering Science 14 (1976) 1135-1142.

APPENDIX

The stress σ_b in the bonding zone was assumed constant in Section 5. Here we shall use the form

$$\sigma_b = \sigma_0 f(\bar{v}) \quad (A.1)$$

where $\bar{v} = (v^+ - v^-)/z_0$, in which σ_0 and z_0 are constants with dimensions of stress and length, respectively. The separation between the surfaces is $v^+ - v^-$. The bond energy is

$$2\gamma_b = z_0 \sigma_0 \int_0^\infty f \, d\bar{v} \quad (A.2)$$

Greenwood and Johnson [12], in a study of adhesive crack growth used

$$f = (1 + \bar{v})^{-3} \quad (A.3)$$

based on experimental and theoretical considerations of the force of attraction between smooth surfaces. Figure 7 shows their predicted distributions of f and \bar{v} for elastic materials, where E_R^+ is defined in (94). Here we will not use (A.3); the only assumption about f we make is that it vanishes rapidly enough with increasing \bar{v} to ensure validity of the Barenblatt method (i.e., a small-scale effective bonding-zone length) and convergence of the relevant integrals. In addition, we shall use the creep compliance (32), but with $D_0 = 0$, and assume as before that the compliance of the material below the bonding surface D^- is proportional that above this surface, D^+ ; hence,

$$E_R^+ D_1^+ = E_R^- D_1^- \quad (A.4)$$

The surface stress in the elastic problem, (27), for quasi steady-state bonding, (31), becomes

$$\sigma_b^R = E_R^+ D_1^+ \sigma_0 \bar{a}_b^{-m} \int_0^\xi (\xi' - \xi)^m \frac{df}{d\xi'} d\xi' \quad (A.5)$$

with $df/d\xi' = df/d\bar{v} \cdot d\bar{v}/d\xi'$. From (24) and (A.4) with $\beta = \infty$,

$$\bar{v} = (v^+ - v^-)/z_0 = \frac{(1-v^2)}{E_R^+ z_0} (1 + D_1^-/D_1^+) \int_0^\infty \sigma_b^R(\xi') F(\xi'/\xi) d\xi' \quad (A.6)$$

Substitute (A.5) into (A.6) and eliminate ξ and ξ' in favor of the dimensionless variable

$$\psi = \psi(\xi) \equiv (D_1^+ + D_1^-) \sigma_c \xi^{m+1} / \dot{a}_b^m z_0^{(m+1)} \quad (A.7)$$

Also, define $\psi' \equiv \psi(\xi')$ and $\psi'' \equiv \psi(\xi'')$; hence,

$$\bar{v} = \int_0^\infty \int_\infty^{\psi'} \left[\left(\frac{\psi''}{\psi'} \right)^p - 1 \right]^m \frac{df}{d\psi''} F[(\psi'/\psi)^p] d\psi'' d\psi' \quad (A.8)$$

Here, $p \equiv 1/(m+1)$. Inasmuch as $f = f(\bar{v})$, this is an integral equation for $\bar{v} = \bar{v}(\psi)$. The primary result for our purposes is that \bar{v} is a function of only the dimensionless variable ψ . This observation together with (A.5) permits us to reduce (28) to

$$K_I^R/E_R^+ = k_2 z_0 (D_1^+ \sigma_0 / z_0 \dot{a}_b^m)^{.5/(m+1)} \quad (A.9)$$

where $k_2 = k_2(m)$ is dimensionless function of only m . By solving for \dot{a}_b the same exponent q as in (56) is obtained. In order to determine the value of k in the power law (56) it would of course be necessary to find k_2 , which requires the solution of (A.8). It should be added that Greenwood and Johnson [12] obtained $\dot{a} \sim K_I^q$ in the crack growth problem where q is the same as in (56).

We may use arguments similar to those in Section 5 to show that (A.9) is valid for a compliance which does not obey a pure power law, as long as $d \log D/d \log t$ is a slowly varying function of $\log t$. However, without further analysis it is not possible to indicate just how slow the variation must be to achieve an acceptable degree of accuracy.

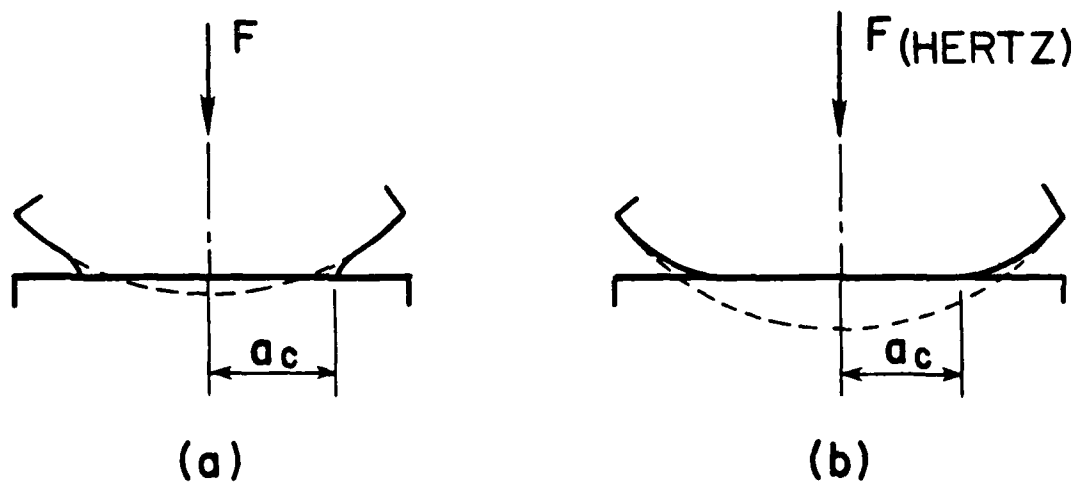


Figure 1. Contact configurations (a) with surface energy and (b) without surface energy. After [12].

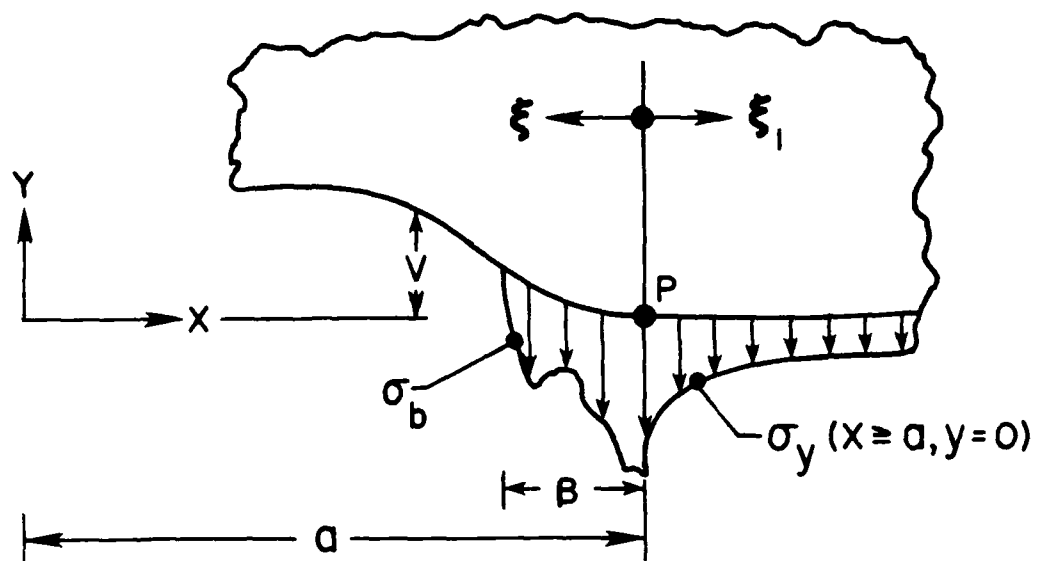


Figure 2. Normal stress and displacement along the bond surface in the neighborhood of the bond edge.

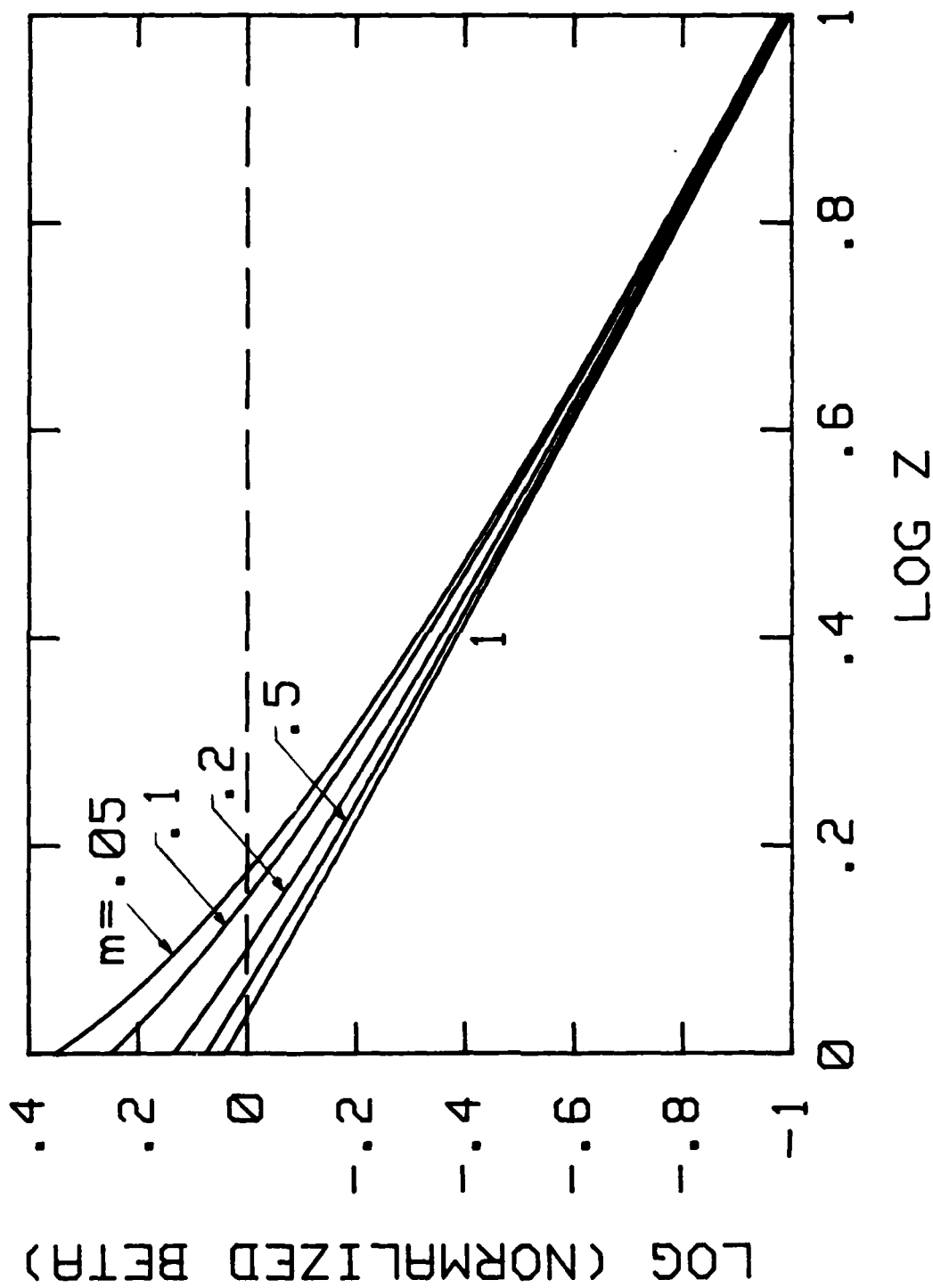


Figure 3. Variation of normalized bonding-zone length with normalized stress intensity factor squared, equations (44) and (49).

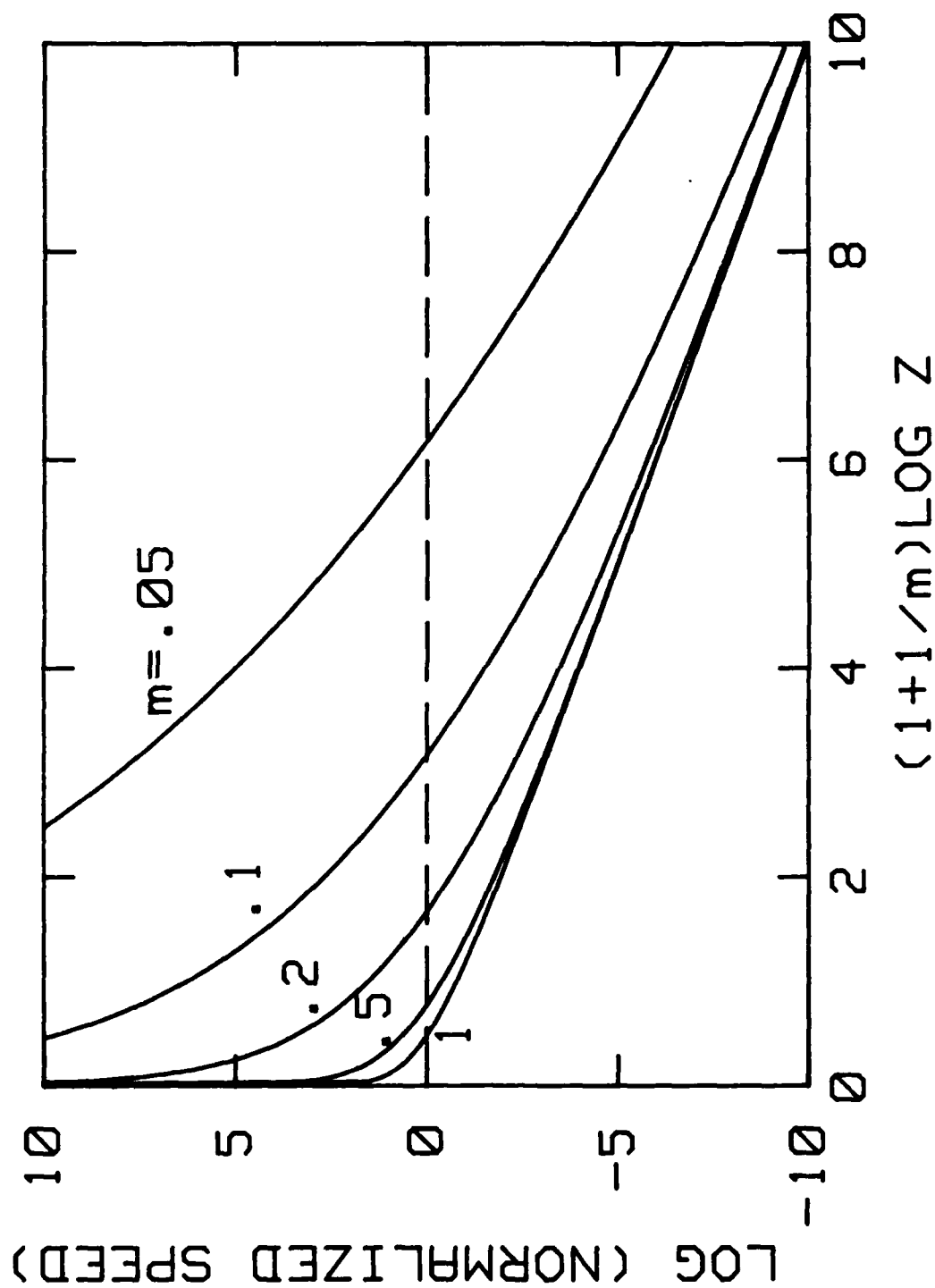


Figure 4. Variation of normalized bonding speed with normalized stress intensity factor squared, equations (46) and (49).

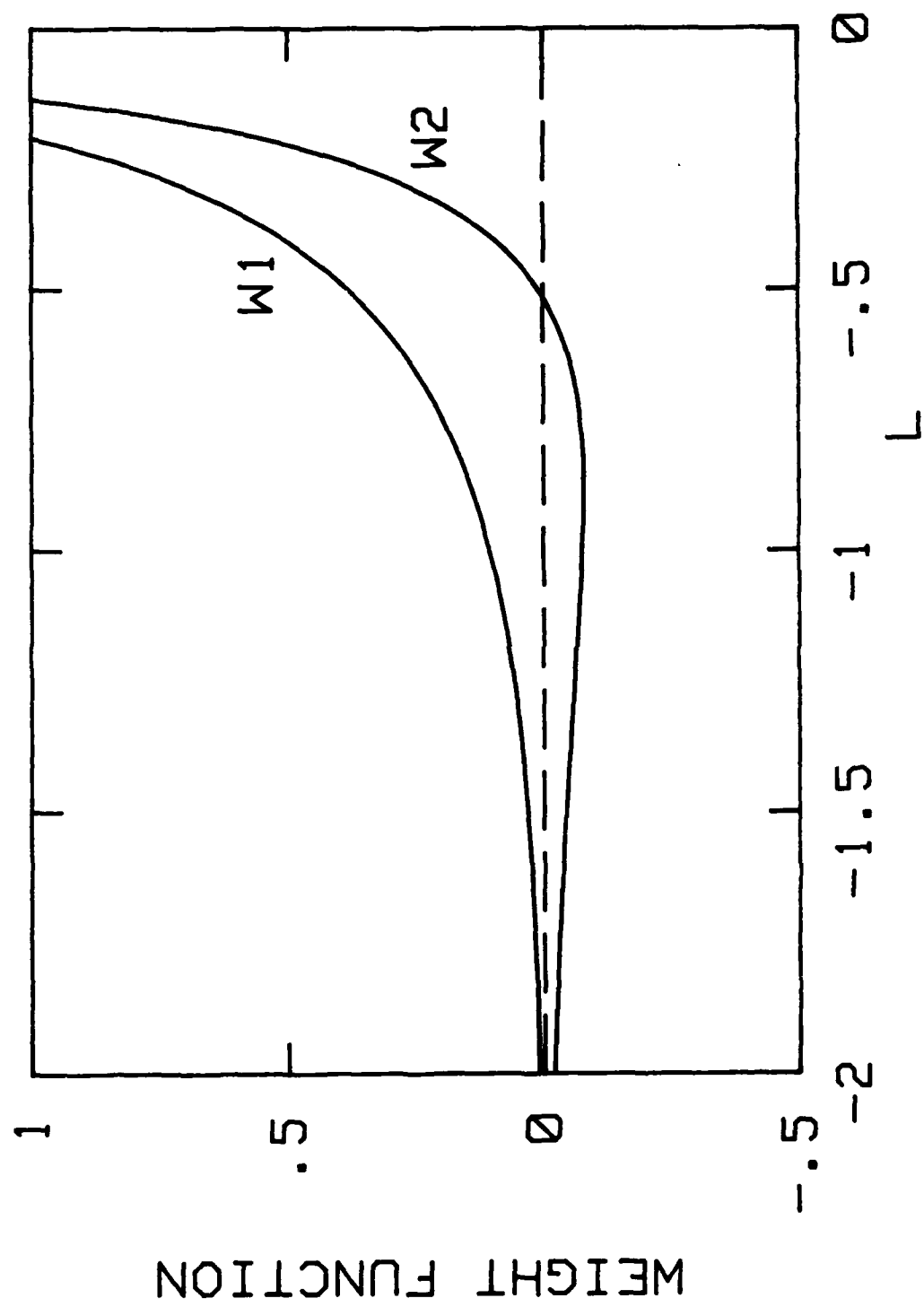


Figure 5. Weight functions, equations (61) and (66).

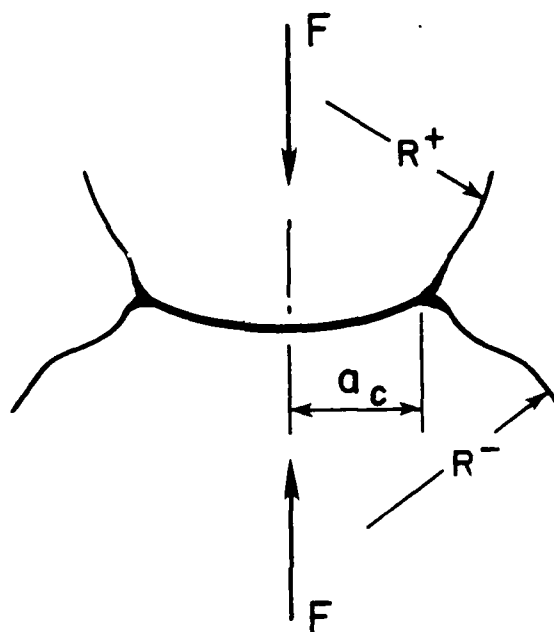


Figure 6. Bonded contact between initially curved surfaces.

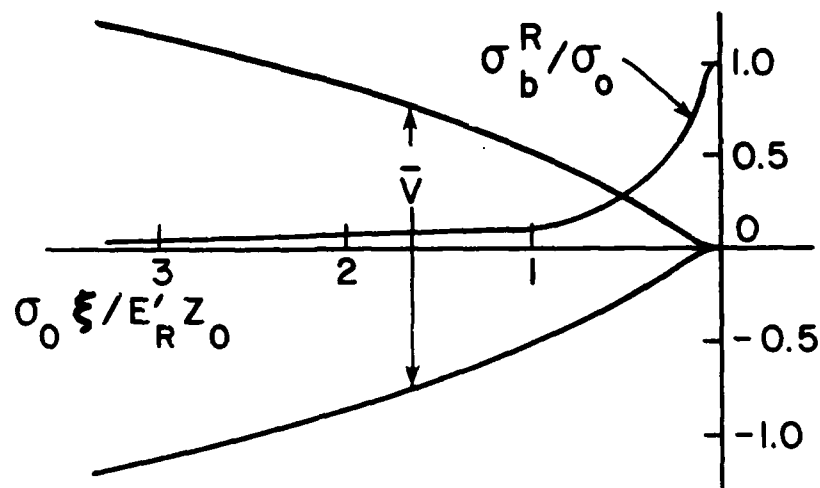


Figure 7. Distributions of bonding stress and separation between surfaces for elastic materials. After [12].